Theoretical predictions of enforced structural changes in molecules

— **Source link**

Krzysztof Wolinski, Jon Baker

Institutions: Maria Curie-Skłodowska University

Related papers:

- Understanding Covalent Mechanochemistry

- First principles dynamics and minimum energy pathways for mechanochemical ring opening of cyclobutene.

- The mechanical strength of a covalent bond calculated by density functional theory

- Mechanochemistry: the mechanical activation of covalent bonds.

- Covalent mechanochemistry: theoretical concepts and computational tools with applications to molecular nanomechanics.

Theoretical predictions of enforced structural changes in molecules

Krzysztof Wolinski, Jon Baker

Theoretical predictions of enforced structural changes in molecules

Theoretical predictions of enforced structural changes in molecules

Krzysztof Wolinski[1,2] and Jon Baker[1]

[1]Parallel Quantum Solutions,

2013 Green Acres Road, Suite A

Fayetteville, Arkansas 72703, U.S.A.

e-mail: baker@pqs-chem.com

[2]Department of Chemistry,

Maria Curie-Sklodowska University,

pl. Maria Curie-Sklodowska 3, 20-031 Lublin, Poland

e-mail: Wolinski@vsop408.umcs.lublin.pl

Abstract

We propose a very simple quantum chemical model to simulate the effect of external forces acting on a single molecule. It involves optimizing the geometry of a molecule with an external force applied to selected nuclei. We use this approach to investigate conformational transitions of the pyranose ring which have been the subject of several atomic force microscopy (AFM) experiments as well as to generate a number of previously unknown isomers of azobenzene.

1

Introduction

In the last two decades a new field in chemistry has opened up; experiments on individual molecules have been performed using scanning probe microscopy (SPM). Manipulations on single molecules involve external forces. A molecule exposed to the stresses caused by external forces changes its geometry; this may even involve the breaking of chemical bonds as well as the formation of new bonds. This new field is often called mechanochemistry.

Many experiments in this area have investigated the mechanical properties of molecules. For systems with a high degree of conformational freedom, single-molecule force spectroscopy (SMFS) permits the study of properties such as the elasticity of polymers with (claimed) piconewton sensitivity and subnanometer accuracy [1]. In particular, the technique of atomic force microscopy (AFM) appears to be very useful in investigating conformational transitions in single molecules. Studies on polysaccharides based on single-molecule manipulations in AFM experiments have shown that the observed elastic deformation is the result of a transition from a chair-like to a boat-like conformation as well as from chair-to-chair inversion in the pyranose ring [2-6]. These conformational transitions have been successfully investigated theoretically via molecular dynamics simulations [6,7].

AFM techniques have also been used to enforce chemical reactions where both bond-breaking and bond formation take place [8,9] and to investigate the rupture of covalent bonds [10]. Scanning Tunneling Microscopy (STM) is another technique that has been used to form new chemical bonds. By using STM on a silver surface a carbon monoxide (CO) molecule was successfully bonded to individual iron (Fe) atoms to form FeCO and $Fe(CO)_2$ [11], as well as to produce CO_2 in reaction with oxygen atoms [12]. Very sophisticated STM experiments have been conducted on copper surfaces where a biphenyl molecule has been formed in reaction with two iodobenzenes [13]. Mechanochemistry on single molecules using a range of different techniques has been reviewed in [14].

In this paper we propose a very simple quantum chemical model to predict structural changes in a molecule exposed to the stresses caused by external forces. This model does not simulate the dynamics of any experiments on single molecules; it just shows what may happen in a molecule if external forces are applied to selected nuclei. Quantum chemistry calculations have been used for this

2

purpose before, e.g., to support the interpretation of AFM measurements [2,3,5,15]. However they have been limited to finding the equilibrium structure of conformers [2,3] or to performing constrained geometry optimizations [5,15].

In [15] the mechanical stretching of a bond was simulated by a series of constrained DFT geometry optimizations with a fixed bond length. The bond distance was increased in small steps and the forces acting on the two atoms involved in the bond were computed. This procedure was continued until the maximum force was found, providing a rough idea of the mechanical bond strength and giving the potential as a function of distance. This information was then used in a simple Arrhenius kinetic model involving a Morse potential with the parameters of the potential determined from the DFT results. This procedure has been given the acronym COGEF (COnstrained Geometries simulate External Force) [15]. In our approach we do not simulate the effects of an external force, rather we apply an external force directly and see what it does.

Theory

The basic idea is to apply a constant and continuous external force to specific nuclei in a molecule during the course of an otherwise standard geometry optimization. External forces acting on selected nuclei give rise to an additional energy term. For consistency between the energy and its gradient it is desired to define this additional potential energy in such a way that the external force is its negative first derivative with respect to the nuclear positions. Thus in our model an external force $\mathbf{f}_A$ acting on a given atom A at position $\mathbf{R}_A$ gives a contribution to the potential energy defined as

$$E_{ext,A} = -\mathbf{R}_A \circ \mathbf{f}_A \qquad (1)$$

This is the simplest possible form of the interaction energy. This definition is at least partially analogous to the interaction of a molecule with an external electric field which is given as a dot product of a dipole moment and a field $\mathbf{F}$. The nuclear part of the dipole moment is a sum of $\mathbf{R}_A * Z_A$ (nuclear coordinates times atomic number). Hence, the contribution to the interaction energy from one nucleus A is given as $-\mathbf{R}_A * \mathbf{F} * Z_A$. Here, the electric field $\mathbf{F}$ rescaled by the atomic number Z_A gives the force acting on nucleus A $\mathbf{f}_A = \mathbf{F} * Z_A$ in eq.(1).

3

The total molecular energy in the presence of external forces is given as

$$E(\mathbf{f}) \;=\; E + E_{ext} \;=\; E - \sum_A \mathbf{R}_A \circ \mathbf{f}_A \tag{2}$$

where $\mathbf{f}$ denotes all external forces (acting on all selected atoms), E is the energy at the current geometry without external forces and the sum runs over atoms to which external forces have been applied. The total force acting on a given atom A is, as usual, given by the negative first energy derivative with respect to atomic coordinates $\mathbf{R}_A$

$$\mathbf{F}_A \;=\; -dE/d\mathbf{R}_A \;=\; -d(E+E_{ext})/d\mathbf{R}_A \;=\; -dE/d\mathbf{R}_A + \mathbf{f}_A \tag{3}$$

The equilibrium geometry of a system with external forces is determined by the condition that

$$\mathbf{F}_A = \mathbf{0} \quad \rightarrow \quad dE/d\mathbf{R}_A = \mathbf{f}_A \quad \text{for each nucleus A} \tag{4}$$

Thus a molecule has to change its geometry in order to generate an internal force which will cancel the external force.

The Hamiltonian of a molecular system under such a perturbation can be written as

$$\mathbf{H} \;=\; \mathbf{H}_0 + \mathbf{H}_1 \;=\; \mathbf{H}_0 - \sum_A \mathbf{R}_A \circ \mathbf{f}_A \tag{5}$$

with $\mathbf{H}_0$ being the Hamiltonian for the unperturbed system. It should be emphasized that the perturbation defined above does not change (influence) the electronic structure of a molecule at a given geometry. As a result, the interaction energy defined by Eqs. (1) and (2) is calculated in a fully classical manner just like for example the nuclear repulsion energy in a molecule (within the Born-Oppenheimer approximation). The total energy (Eq. (2)) and its gradient are calculated quantum mechanically. In general, this perturbation will enforce geometry changes.

In the proposed model external forces can be applied to an arbitrary number of nuclei in arbitrary directions. However, if the total external force is not zero then the whole molecule will

4

translate. In the case of the total torque not being zero a molecule could also rotate. However, in these studies we apply the external force along a line joining pairs of atoms in a molecule, either as a "push" (to push the two atoms together) or as a "pull" (to pull them apart). Whatever force is applied to one of the two atoms, an equal and opposite force is applied to the other atom. This ensures that there is no net force on the molecule and thus no tendency for the system to translate or rotate. In effect, the molecule will remain in place under simulated pressure.

In the particular case of equal but opposite forces applied to two atoms, i.e., $\mathbf{f}_A=-\mathbf{f}$ and $\mathbf{f}_B=+\mathbf{f}$ the total interaction energy from eq.(1) is given by

$$E_{ext} = - (\mathbf{R}_B - \mathbf{R}_A) \circ \mathbf{f} \qquad (6)$$

The external force $\mathbf{f}$ acts along the line joining atoms A and B, i.e., in the direction

$$\mathbf{d} = (\mathbf{R}_B - \mathbf{R}_A)/R_{BA} \qquad (7)$$

and is defined as

$$\mathbf{f} = \mathbf{d}*f \qquad (8)$$

where f denotes the magnitude of the external force $\mathbf{f}$ and R_{BA} is the norm of the $(\mathbf{R}_B - \mathbf{R}_A)$ vector. Substituting (7) and (8) into eq.(6) gives a total interaction energy of

$$E_{ext}= -R_{BA}*f \qquad (9)$$

and the total molecular energy in the presence of external forces (2) is

$$E(f) = E - R_{BA}*f \qquad (10)$$

It is easy to check that derivatives of E_{ext} yield the external forces applied to atoms A and B

$$-dE_{ext}/d\mathbf{R}_A =+dR_{BA}/d\mathbf{R}_A * f = - (\mathbf{R}_B - \mathbf{R}_A)/R_{BA} * f = - \mathbf{d} * f = - \mathbf{f} = \mathbf{f}_A$$

$$-dE_{ext}/d\mathbf{R}_B =+dR_{BA}/d\mathbf{R}_B * f = +(\mathbf{R}_B - \mathbf{R}_A)/R_{BA} * f = +\mathbf{d} * f = + \mathbf{f} = \mathbf{f}_B$$

5

Thus the theory our method is based on is fully consistent. It should be noted that in the above example the external force applied to two atoms is constant only in terms of its magnitude f. The direction of the force **f** depends on the nuclear positions and thus changes in every geometry optimization cycle. In all calculations reported in this paper the external forces have been handled according to eqs. (7), (8) and (6).

The theory presented above is in some ways rather formal. The additional energy term (1) representing the interaction of a molecule with the external force(s) does not change the geometry optimization algorithm. In practical terms, during a geometry optimization an additional gradient for the two atoms in question is added to the standard gradient vector computed for the entire molecule. Given that the main factor determining the next step in the optimization algorithm is the gradient vector, then the optimization will proceed in exactly the same way whether the additional energy term is included or not. For energy comparisons with structures obtained *without* the application of an external force it is probably best to leave it out. However, inclusion of this term ensures consistency between the total energy and its gradient. It is also necessary to include the interaction energy term if the main goal is to analyze the potential energy surface (PES) in the presence of external forces. However, in this study, we concentrate on the final structural changes when external forces act on selected nuclei in a molecule. Nevertheless, in all calculations performed here the extra interaction energy term (1) has been included.

The approach we propose here is static in nature, i.e., it does not describe how structural changes take place in a molecule when external forces act on selected nuclei. Consequently it cannot simulate the dynamical processes that occur during an AFM experiment. This can be done only by molecular dynamics calculations [7]. However, our model does allow us to predict the final outcome of an AFM experiment. (In other words we can predict what happens but not how it happens.)

As mentioned in the Introduction the model proposed here is closely related to the COGEF method [15]. While COGEF predicts what forces would be needed to, say, elongate a molecule by increasing the distance between two selected atoms, in our approach an explicitly given external force applied to two atoms elongates a molecule. These two approaches are equivalent, i.e., both yield the same structure for the same (implicit and explicit) applied force. If the force f acting on atoms A and B,

6

derived from a COGEF calculation with a fixed distance, R_{BA}, between these atoms is used in our method it results in an identical structure. This is obvious from eq. (10) where, in this case, E is just the COGEF energy of a molecule with fixed R_{BA}. Thus there is correspondence between the R_{BA} distance fixed in COGEF and the external force applied in our model. Note, however, that this is true only up to the maximum COGEF force (the force required to break the bond), in our approach, if external forces greater that this maximum are applied then typically the system simply breaks apart, whereas a constrained geometry optimization can be successfully carried out at distances R_{BA} greater than the distance corresponding to the maximum COGEF force.

Applications

The theoretical model proposed above has been utilized in this work in both the "pulling" and "pushing" modes. The pulling mode has been used to examine possible conformational changes in the pyranose ring while the pushing mode has been applied to *cis*-azobenzene to generate new structural isomers.

The standard level of theory adopted throughout this work was Density Functional Theory [17] using the B3LYP exchange-correlation functional [18] and the 6-31G* basis set [19]. Structures located at this level of theory for azobenzene were subsequently refined at MP2/6-311G** to ensure that the energetics (relative energies and barrier heights) remained stable. All geometry optimizations used our standard convergence criteria, i.e., the maximum residual force on any atom must be less than 0.0003 au and *either* the maximum atomic displacement must be less than 0.0003 au *or* the energy change from the previous cycle must be less than 0.000001 au. All calculations reported in this paper have been performed in parallel with the PQS program package [19]. Structural changes have been visualized and analyzed using our Graphical User Interface (GUI), PQSMol [19].

External forces were applied to two selected nuclei in each molecule. The applied external forces act along the line connecting the two atoms and either pulled them in opposite directions (pyranose ring) or pushed them together (*cis*-azobenzene). All our calculations with external forces started from the optimized ground state geometries. The magnitude of the applied force had to be adjusted for each system. The force required to induce permanent geometrical changes is obviously

7

related to the reaction barrier height. Forces which are too small will only elongate or shorten some bonds without any transition. On the other hand, too large forces could break a molecule apart. For example, our calculations showed that there is, above a given minimum, a fairly wide range of external forces that cause the chair-to-boat transitions in the pyranose ring. We have attempted to find the minimum force but its magnitude was only roughly optimized.

Pyranose ring

The conformational transitions of the pyranose ring have been the subject of several AFM experiments on single polysaccharide molecules reported by Marszalek *et al.* [2,3]. It was demonstrated in these studies that stretching single pectin molecules results in changes in the conformation of the pyranose ring. These changes include the chair-to-boat transition as well as the chair-to-chair inversion. The latter is seemingly a two-step chair-to-boat-to-chair process [3]. A major role in these transitions is played by the two glycosidic bonds which act as mechanical levers generating a torque when a force is applied to linkage oxygens. However, only axial glycosidic bonds generate a non-zero torque which causes a rotation around the C-O or C-C bonds in the pyranose ring [3].

One of the goals of this work was to investigate and describe possible conformational transitions of the pyranose ring under the stress caused by external forces. We have considered a simple model: the pyranose ring with two glycosidic bonds ($C_5H_{10}O_3$) as shown in Fig. 1(a1). The pyranose ring can have the chair or the boat conformation and the glycosidic bonds may remain in the axial (a) or the equatorial (e) positions. This, in general, yields four possible chair and boat conformers of $C_5H_{10}O_3$. It should be emphasized, however, that there are a number of structures close in energy for each of these conformers, for example differing by the hydroxyl hydrogen flip. In addition, polymers can be formed through the glycosidic bonds by elimination of water.

We have considered three pyranose-based monomers HO-(C_5H_8O)-OH and three dimers HO-($C_5H_8O_3$)-O-($C_5H_8O_3$)-OH with different conformations. The monomers Oa-Chair-Oe, Oe-Chair-Oa and Oa-Chair-Oa are shown in Fig. 1, (a1), (a2) and (a3), respectively, and the dimers Oa-Chair-Oa-Chair-Oa, Oa-Boat-Oa-Chair-Oa and Oa-Boat-Oa-Boat-Oa are presented in Figures 2, (a1), (a2) and

(a3), respectively. In all cases a constant magnitude force has been applied as described previously to the terminal glycosidic oxygens. These forces act along the line connecting both oxygens and pull them in opposite directions.

Chair-to-Boat Transition

We begin with the chair-to-boat transition. We have investigated two such cases with the chair conformer having the glycosidic bonds in the axial (a) and equatorial (e) positions: Oa-Chair-Oe and Oe-Chair-Oa. They are shown in Fig. 1, (a1) and (a2), respectively. Pulling the two glycosidic oxygens with a force of 0.025 au (~2060 pN) results in transitions to Oe-Boat-Oe conformations, Fig. 1 (b1) and (b2), respectively. In both cases the linkage of the pyranose ring with the glycosidic bond in the axial position flips. (This is described as rotating around the imaginary ring C-O axis by Marszalek *et al*. [3]). The equatorial side stays essentially unchanged. The final boat structures are slightly different in energy for the two cases. The elongation of each molecule measured by the distance between the glycosidic oxygens R_{O-O} [2-6] is shown in Figure 1. In both cases this elongation is about 24% with respect to the chair conformer.

If the two Oe-Boat-Oe conformers are allowed to relax, i.e., are reoptimized with no applied force, then the second Oe-Boat-Oe conformer remains intact with some minor geometrical changes. However, in the first case, reoptimization results, surprisingly, in another transition: both linkages of the pyranose ring in the Oe-Boat-Oe conformer flip down (rotating around the imaginary C-C and C-O axes, respectively) to form the Oa-Boat-Oa conformer as shown in Fig. 1(c1). The final relaxed Oa-Boat-Oa structure is some 3 kcal/mol lower in energy than the Oe-Boat-Oe conformer from the second case.

Chair-to-Chair Inversion

This process occurs only with the chair pyranose ring having both glycosidic bonds in the axial positions. Pulling the two glycosidic oxygens of the Oa-Chair-Oa conformer with a force of 0.050 au (~4120 pN) causes inversion to the Oe-Chair-Oe conformation. This is shown in Fig. 1, (a3) and (b3). It should be emphasized that a single applied force (of magnitude 0.050 au.) causes the flipping of both

9

linkages of the ring. Thus according to our calculations, this is a one-step process resulting in a molecular elongation of about 31%. This is in contrast to the conclusion in [3] where the two observed elongations of the polysaccharide in the AFM experiment were attributed to two consecutive one-side transitions caused by two different forces: Oa-Chair-Oa – f1 → Oe-Boat-Oa – f2 → Oe-Chair-Oe. However, the molecule on which the AFM experiments were performed was unlikely to be single monomer [3]. Consequently we decided to investigate the possibility of finding two-step transitions in dimers.

Transitions in Dimers

Three dimers with pyranose rings in the chair-chair, boat-chair and boat-boat conformations are shown in Fig. 2, (a1), (a2) and (a3), respectively. They all have three gycosidic bonds in the axial position. We started our search for conformational changes using relatively small forces applied to the two terminal glycosidic oxygens in the same way as in the monomers and then increased the applied force gradually until a transition occurred.

The first Oa-Chair-Oa-Chair-Oa dimer transformed into an Oe-Chair-Oe-Chair-Oe conformation in one step when a force of 0.057 au (~4697 pN) was applied. The molecule elongates (elongation measured as a distance between the terminal glycosidic oxygens) from 8.693 Å to 11.782 Å, i.e., by 35.5%, and its energy increased significantly by 33.6 kcal/mol. Relaxation does not change the molecular conformation but results in a significant energy lowering of 36.7 kcal/mol. Thus the final relaxed Chair-Chair structure with equatorial glycosidic bonds is 3.1 kcal/mol lower in energy than the starting conformer with axial bonds. This is shown in Fig. 2, (a1), (b1) and (c1).

Two-step transitions do occur in the other two dimers. The Boat-Chair and Boat-Boat conformers with all axial glycosidic bonds undergo a two-step transformation into distinct Chair-Chair conformers with all equatorial bonds. In both cases significantly different forces were needed to induce the transitions. The intermediate conformations were also different in the two cases, however, in both cases the first transition transforms one axial Oa-Boat-Oa of the dimer into an equatorial Oe-Chair-Oe. In the second step the remaining boat transforms into a chair (second case) and all remaining axial glycosidic bonds change to equatorial. This is shown in Figs. 2, (a2)-(d2) and (a3)-(d3).

10

The forces required to initiate the first transition were 0.004 au (~330 pN) for the Boat-Chair dimer and 0.002 au (~165 pN) for the Boat-Boat. The second transition occurred at substantially different applied forces of 0.050 au (~4120 pN) and 0.005 au (~412 pN), respectively. The elongation in the Boat-Chair dimer was 117.5% (from 5.358 Å to 9.978 Å and then to 11.656 Å). Elongation in the Boat-Boat dimer was an even greater 258.9% (from 2.966 Å to 7.857 Å and then to 10.644 Å).
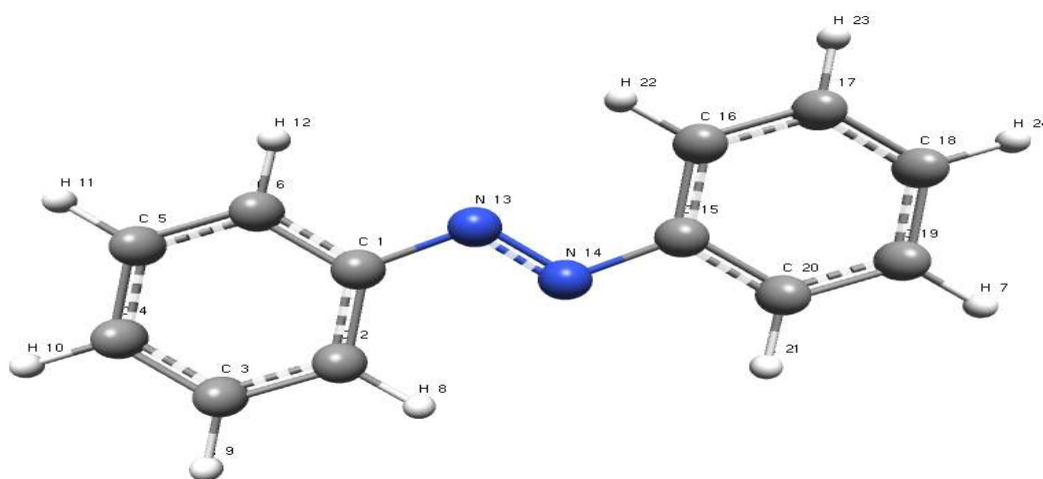
The energetics of these transitions also differed significantly in the two cases. For the Boat-Chair dimer the first and the second transitions changed the energy by +6.8 and +25.6 kcal/mol, respectively. For the Boat-Boat dimer, the first transition resulted in essentially no change in energy, while the second transition increased the energy by +5.9 kcal/mol.

Relaxation of the final enforced Oe-Chair-Oe-Chair-Oe structures took different paths for the two dimers. In the first case (Fig. 2, (a2)-(d2)) some relatively minor geometrical changes occurred leaving the molecule in the same conformation with the energy lower by 28.7 kcal/mol. In the second case (Fig. 2, (a3)-(d3)), relaxation was accompanied by transition to the Boat-Boat conformation with all axial glycosidic bonds, i.e., back to the original conformer. This was accompanied by a reduction in energy of about 10.9 kcal/mol. Thus in this case the mechanically induced transition appears to be reversible.

We would like to comment on the magnitude of the forces needed in our model to induce the conformational transitions described above. In the case of one-step transitions in both monomers and dimers they are about 2-4 times higher than forces used in real AFM experiments (which are up to 1500 pN [3]). These discrepancies are mainly due to weaknesses in our simple approach (see the Note at the end of this paper) but may also result from the use of inappropriate molecular models. The model monomers used in our calculations are too small and rigid compared to the molecules used in the AFM experiments. The latter conclusion seems to be supported by the results obtained here for the two-step transition of the Oa-Boat-Oa-Boat-Oa dimer where forces of only a few hundred piconewtons (165 and 412 pN) were required.
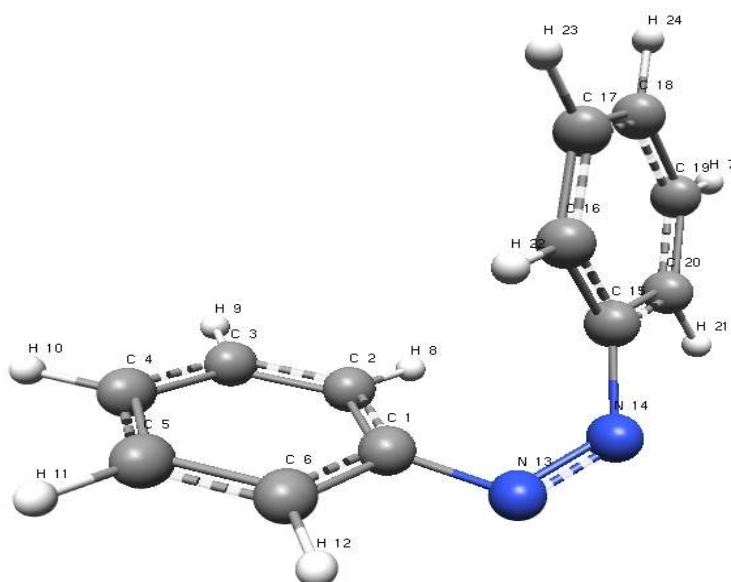
Azobenzene

11

Azobenzene is depicted schematically below. The most stable configuration is the *trans* form (C_{2h}), but there is also a *cis* form (C_2) which is around 15 kcal/mol higher in energy (B3LYP/6-31G*). The barrier height, relative to the *trans* conformer, is a fairly substantial 40.5 kcal/mol. (Experimentally these values are around 12 and 47 kcal/mol, respectively [20].)

trans-azobenzene

cis-azobenzene

12

Azobenzene has already been the subject of AFM experiments and is under study as a potential "molecular machine" in future nanoscale devices [21]. The *cis* ↔ *trans* conversion can be induced optically, and involves a substantial change in the "end-to-end" distance in the molecule.

Originally our aim was simply to reproduce the *cis* ↔ *trans* conversion observed in AFM experiments, but we found that, by directing external forces along vectors connecting two carbon atoms in *cis*-azobenzene, one in each of the two benzene rings, so as to push the atoms together, we could induce bond formation and produce a number of different "fused ring" and other products. These were all stable after removal of the applied force and reoptimization.

We found five different "fused ring" structures, at least two of which have chiral equivalents, plus two biphenyl-like species with N_2 attached to one of the rings. All structures found are shown in Fig. 3. Table 1 gives the energies of all these structures, relative to *cis*-azobenzene, at both B3LYP/6-31G* and MP2/6-311G**, together with the two carbon atoms defining the direction of the applied force and the number (and location) of new bonds formed. Transition states between each product and *cis*-azobenzene were located in separate calculations and their relative energies are also shown. All stationary points were characterized by a full vibrational analysis. Examination of the CAS scientific literature data base (searched using the empirical formula) revealed probably over 1000 different structural isomers with formula $C_{12}H_{10}N_2$, but those shown in Fig. 3 were either completely absent or present but with no reported references.

The external force required to cause the various reactions in *cis*-azobenzene was between 0.06 and 0.10 au (~4900 to 8200 pN), significantly more than that required to induce the conformational changes in the pyranose ring, discussed earlier. These forces are about an order of magnitude higher than used in current AFM experiments, indicating that the new isomers are unlikely to be formed under current experimental conditions.

All of the new isomers of $C_{12}H_{10}N_2$ show substantial barriers to their formation from *cis*-azobenzene (a minimum of 55.6 kcal/mol at B3LYP/6-31G*, falling slightly to 47.0 kcal/mol at MP2/6-311G**) with in most cases much lower barriers for the reverse reaction. In all cases a new bond is formed between the atoms defining the applied force; additionally in three of the "fused ring"

13

structures a second bond forms between two other ring atoms.

Surprisingly, the most stable of the new isomers, both thermodynamically and kinetically, are the two in which at least one C-N bond has been broken. These involve a biphenyl-like structure with N_2 attached to one of the rings either linearly (Fig.3(a)) or side-on (Fig.3(b)). The linear structure lies (MP2/6-311G**) just 11.0 kcal/mol above *cis*-azobenzene and has a reverse barrier height of 36.0 kcal/mol; at B3LYP/6-31G* the reverse barrier height is an even higher 42.6 kcal/mol. The energetic relationship between this structure and *cis*-azobenzene is thus quite similar to that between the latter and its *trans*-conformer, and suggests quite strongly that it may survive experimentally assuming that it can be formed in the first place.

The structure with the side-on N_2 is 20.7 kcal/mol higher in energy than *cis*-azobenzene at the MP2 level (28.0 kcal/mol at B3LYP); however it has a huge barrier for the rearrangement of over 90 kcal/mol. This is not surprising given that it involves the largest structural distortion relative to *cis*-azobenzene of all the new isomers. The high forward barrier also means that it has the highest reverse barrier (64 kcal/mol at B3LYP/6-31G*) and so is kinetically the most stable isomer, at least as far as rearrangement back to *cis*-azobenzene is concerned. Unlike most of the other species it has symmetry (C_s). (The barrier height for rotation of the phenyl ring (by 180º) is ∼5 kcal/mol at both MP2 and B3LYP, and the transition state also has C_s symmetry, as befits a 90º rotation.) Note, however, that despite an extensive search, we were unable to locate the transition state for this reaction at MP2/6-311G**. Normally the MP2 optimization, starting from the converged B3LYP/6-31G* structure and Hessian, converged rapidly; not so in this case. This does place a question mark over the kinetic stability of the side-on N_2 isomer (Fig.3(b)), although there is no doubt that it is a minimum on both potential energy surfaces.

The next most stable isomer is the structure shown in Fig.3(c), which has C_2 symmetry and lies 26.8 kcal/mol above *cis*-azobenzene, with a reverse barrier height of 25.4 kcal/mol (MP2/6-311G**). At the B3LYP level, this is actually marginally more stable thermodynamically than the side-on N_2 isomer although its kinetic stability is lower.

The remaining four "fused-ring" isomers are much less stable. There are significantly higher in

14

1
2
3
4
5
6
7
8
9
10
11
12
13
14
15
16
17
18
19
20
21
22
23
24
25
26
27
28
29
30
31
32
33
34
35
36
37
38
39
40
41
42
43
44
45
46
47
48
49
50
51
52
53
54
55
56
57
58
59
60

energy thermodynamically with much lower reverse barrier heights; around 12 kcal/mol for the two most stable structures (Fig.3(d) and Fig.3(e)), and 5-6 kcal/mol for the other two. The new C-C bonds formed in these isomers are longer and weaker than in the more stable structures (see Table 1).

15

Table 1 Energies (kcal/mol) of the various isomers of azobenzene and their transition states (relative to *cis*-azobenzene) and the ring carbon atoms defining the direction of the applied force

Structure	Applied Force[1]	New Bonds (length in Å)			B3LYP/ 6-31G*	MP2/ 6-311G**
			B3LYP	MP2		
Fig. 1(a)	C2 – C15	C2-C15	1.533	1.521	15.5	11.0
TS					58.1	47.0
Fig. 1(b)	C4 – C15	C4-C15	1.533	1.524	28.0	20.7
		N14-C1	1.499	1.500		
TS					92.3	----[2]
Fig. 1(c)	C2 – C16	C2-C16	1.543	1.535	27.3	26.8
TS					55.6	52.2
Fig. 1(d)	C4 – C19	C4-C19	1.607	1.596	58.4	39.6
		C1-C20	1.565	1.563		
chiral	C4 – C17	C4-C17; C1-C15				
TS					72.0	51.7
Fig, 1(e)	C3 – C17	C3-C17	1.626	1.609	68.4	50.0
		C6-C16	1.574	1.570		
TS					79.2	61.6
Fig. 1(f)	C4 – C20	C4-C20	1.659	1.649	67.4	56.4
chiral	C4 – C16	C4-C16				
TS					73.7	61.2
Fig. 1(g)	C3 – C20	C3-C20	1.639	1.628	78.6	59.3
		C6-C15	1.579	1.571		
TS					84.6	64.0

[1] force applied so as to push the two indicated carbon atoms together

[2] the MP2 transition state could not be located

Perhaps the best way of detecting any of these new isomers is by vibrational spectroscopy. Simulated IR and Raman spectra of *trans*-azobenzene, *cis*-azobenzene and all seven of the new isomers are shown in Figs. 4 and 5, respectively. These were obtained from B3LYP/6-31G* force constant matrices which were scaled using the precomputed SQM scale factors taken from ref. [22]. The scale factors relevant to azobenzene and its structural isomers are shown in Table 2.

16

Table 2 Standard B3LYP/6-31G* SQM scale factors relevant to $C_{12}H_{10}N_2$ isomers

Type		Scale factor
stretch	r_{CC}, r_{CN}, r_{NN}	0.9207
stretch	r_{CH}	0.9164
bend	$\angle_{CCC}$, $\angle_{CCN}$, $\angle_{CNN}$	1.0144
bend	$\angle_{CCH}$	0.9431
torsion	all	0.9523
linear bends*	$\angle_{NNC}$	0.8847

* only for isomer C2-C15 (Fig.3(a))

Scaling the Hessian matrix via the SQM procedure typically results in much better agreement with experimental spectra. We must, however, place a health warning on the spectra of the first two isomers (Fig.3(a) and Fig.3(b)) as these contain structural motifs, namely the unusual N_2 arrangements, that were not considered when the set of standard SQM scale factors were derived [22], and so vibrational modes involving significant motion of the nitrogen atoms may be more in error than other modes. Even here, though, agreement should be better with scaling than with the raw, unscaled spectra.

The C2-C15 isomer (Fig.3(a)) has a very intense band at ~2083 cm⁻¹ in the IR spectrum primarily due to a combination of C-N and N-N stretches (Fig.4(c)). There are no bands at all in this region of the IR spectrum for either *trans*- or *cis*-azobenzene, or for any of the other new isomers either, so this is a very strong distinguishing feature. It is predicted to be some 8-10 times more intense than any other band in the IR spectrum of any of the other isomers.

Similarly, although nowhere near as intense, the C4-C15 isomer (Fig.3(b)) has two fairly intense IR active bands at ~1645 and ~1687 cm⁻¹, again mainly due to N-N stretches, which could possibly be used to detect this species (Fig.4(d)).

In the case of C2-C16 (Fig.3(c)), the distinguishing feature here is the very intense band at ~1478 cm⁻¹ in the Raman spectrum (yet again due primarily to a combination of C-N and N-N stretches; Fig.5(e)). The only other isomer with anywhere near as intense Raman bands is *trans*-azobenzene, but at ~1216 and ~1659 cm⁻¹, these straddle the predicted band in C2-C16.

17

The remaining four "fused ring" isomers have very similar spectra to one another, both IR and Raman, and as they are less stable, both thermodynamically and kinetically, than the other isomers, we do not discuss them further.

Given that any signals from the new isomers may well be swamped by those from the more stable *cis*- and, especially, *trans*-azobenzene, a better chance of detecting them might be via vibrational circular dichroism (VCD). A significant advantage of this technique is that *trans*-azobenzene (which after all is the most stable form), being planar, formally has no VCD spectrum. The VCD spectra of *cis*-azobenzene and the seven new isomers are shown in Fig. 6.

The most stable of the new isomers, C2-C15, should be readily distinguishable from *cis*-azobenzene – and all the other species as well – by the strong band at ~2083 cm^{-1} in the simulated VCD spectrum (Fig.6(c)). (This is the same vibration that gives rise to the intense band in the IR spectrum.)

Yet another spectroscopic technique that could be used to detect the new isomers is nuclear magnetic resonance (NMR). The different chemical environments of the nitrogen atoms in the various isomers should lead to substantially different chemical shifts in ^{15}N NMR spectra – and indeed this is exactly what is predicted (see Table 3). The three most stable of the new isomers should be distinguishable by their large positive ^{15}N NMR chemical shifts relative to both *trans*- and *cis*-azobenzene.

18

Table 3 Predicted B3LYP/6-31G* ^{15}N NMR chemical shifts (absolute) for the various $C_{12}H_{10}N_2$ isomers

compound	^{15}N chemical shift		difference from *trans*-azobenzene	
	N_{13}	N_{14}	N_{13}	N_{14}
trans	-261.86	-261.86	0.0	0.0
cis	-302.34	-302.34	-40.48	-40.48
C2-C15	-49.49	-216.34	+212.37	+45.52
C4-C15	-221.74	-221.74	+40.12	+40.12
C2-C16	-112.37	-112.37	+149.49	+149.49
C4-C19	-259.99	-252.80	+1.87	+9.06
C3-C17	-263.57	-276.17	-1.77	-14.31
C4-C20	-155.86	-130.63	+106.0	+131.23
C3-C20	-249.87	-271.24	+11.99	-9.38

Applying larger external forces than the ~4500 to 6600 pN required to induce the isomerization reactions can break *both* of the C-N bonds. By applying a force of 9000 pN directed along carbon atoms C3 and C15 and carefully optimizing, we were able to cause decomposition with loss of molecular nitrogen.

19

Conclusions

We have proposed a very simple quantum chemical method which enables us to mechanically induce structural changes in molecules by applying external forces to selected nuclei. A molecule responds to this external stress by changing its geometry. Optimizing the geometry of a molecule in the presence of appropriate external forces may yield new chemical structures.

In this study we have shown that "pulling" the two oxygens in a glycosidic bond connected to a pyranose ring results in chair-to-boat transitions and chair-to-chair inversion of the ring. Such conformational changes have been proposed in AFM experiments on single polysaccharide molecules and have been explained by the axial glycosidic bonds working as levers [2,3]. Our calculations have confirmed that glycosidic bonds in axial positions are indeed responsible for these conformational changes. It has also been proposed as a result of AFM experiments that the chair-to-chair inversion is a two-step process involving chair-to-boat-to-chair transitions [3]. Our calculations have shown, however, that the inversion process of chair-like conformers takes place (for both monomers and dimers) in a single step i.e., both linkages of the ring flip simultaneously under a single applied force. Two-step transitions occurred only in the case of dimers containing at least one boat unit.

Applying our method in "push" mode to *cis*-azobenzene we have discovered a number of apparently previously unknown isomers of $C_{12}H_{10}N_2$. Selecting different pairs of carbon atoms (one from each of the two benzene rings in *cis*-azobenzene) and pushing them together we have obtained seven new structures. In all cases new chemical bonds have been formed. Five of the new isomers have "fused ring" structures, at least two of which have chiral images. According to our calculations all seven new isomers are at least metastable and three of them should be sufficiently stable kinetically to be observable. We have provided theoretical IR, Raman and VCD spectra as well as nitrogen NMR chemical shifts which may help to identify them in future.

It would be very hard to analyze these kinds of structural changes without a graphical interface capable of visualizing all conformers. The PQSMol interface allowed us to do this in a very easy and convenient way. We encourage interested readers to use the link given in the appendix of this paper to see animations of the conformational changes described in this article.

20

The approach we have used of optimizing structures in the presence of an applied external force is a very simple one and it is surprising to us that it has not been widely used previously. In contrast to most quantum chemical projects where the numerical implementation is usually a major task requiring heavy and demanding coding, the programming effort required to implement the application of external forces was essentially trivial.

After preparing this manuscript for publication we found two closely related papers that have just been published [23,24]. In both, an external force acting along a line connecting two atoms has been explicitly introduced, the same as in this work, and the corresponding force-modified PES discussed. In [23] this approach was used in *ab inito* molecular dynamics simulations of the ring opening in cyclobutene. In [24] the force-modified PES was analyzed for the ring-opening reaction in benzenocyclobutenes.

Note

The model proposed here is very simple and clearly does not fully reflect the physics involved in a real experiment, i.e., the actual interaction between a probe tip and a tethered molecule, which must involve the electron density. We have recently developed a more physical, revised model which maintains the relative simplicity of this model but also affects the electrons. Results with our revised model reproduce those presented here but at significantly lower applied external forces which agree far better with forces found in actual AFM experiments. Our revised model will be presented in a later paper.

Appendix

Many of the conformational changes described here may be visualized at the following URL: http://www.pqs-chem.com/demo/afm.

21

References

1   J. Gimzewski, C. Joachim, *Science* **283** (1999) 1683-1688

2   P. E. Marszalek, A. F. Oberhauser, Y. P. Pang, J. M. Fernandez,
    Nature **396** (1998) 661-664

3   P. E. Marszalek, Y. P. Pang, H. Li, J. E. Yazal, A. F. Oberhauser, J. M. Fernandez,
    Proc. Natl. Acad. Sci. USA **96** (1999) 7894-7898

4   P. E. Marszalek, H. Li, A. F. Oberhauser, J. M. Fernandez,
    Proc. Natl. Acad. Sci. USA **99** (2002) 4278-4283

5   P. E. Marszalek, A. F. Oberhauser, H. Li, J. M. Fernandez,
    Biophys. J. **85** (2003) 2696-2704

6. G. Lee, W. Nowak, J. Jaroniec, Q. Zhang, P. E. Marszalek,
    Biophys. J. **87** (2004) 1456-1465

7. B. Heymann, H. Grubmuller, *Chem. Phys. Lett.*, **305** (1999) 202-208

8. R. Szostakiewicz, S.R.K. Ainavarapu, A.P.Wiita, R. Perez-Jimenez, J.M. Sanchez-Ruiz, J.M.
    Fernandez, *Langmuir*, **24**, 1356-1364, (2008)

9. S.R.K. Ainavarapu, A.P.Wiita, L. Dougan, E.Uggerud, J.M. Fernandez,
    J. Am. Chem.Soc., **130**, 6479-6487, (2008)

10. M. Grandbois, M. Beyer, M. Rief, H. Clausen-Schaumann, H.E. Gaub,
    Science, **283**, 1727, (1999)

11. H. J. Lee, W. Ho, *Science*, **286**, 1719, (1999)

12. J. R. Hahn, W. Ho, *Phys. Rev. Lett.*, **87**, 166102, (2001)

13. S.W. Hla, L. Bartels, G. Meyer, K.H. Rieder, *Phys. Rev. Lett.*, **85**, 2777, (2000)

14. M. Beyer, H. Clausen-Schaumann, *Chem. Rev.* **105**, 2921-2948, (2005)

15. M. Beyer, *J. Chem. Phys.* **112** (2000), 7307

16. P. Hohenberg, W. Kohn, *Phys. Rev. B* **136** (1964) 864;
    W. Kohn, L. J. Sham, *Phys. Rev. A* **140** (1965) 1133

17. A. D. Becke, *J. Chem. Phys.* **98** (1993) 5648

18. R. Krishnan, J. S. Binkley, R. Seeger, J. A. Pople, *J. Chem. Phys.* **72** (1980) 650

19. PQS version 4.0 beta, PQSMol version 1.2-18, *Parallel Quantum Solutions*, 2013 Green Acres
    Road, Fayetteville AR, 72703; http://www.pqs-chem.com ; sales@pqs-chem.com

20. URL : en.wikipedia.org/wiki/Azobenzene

22

1
2
3
4
5
6
7
8
9
10
11
12
13
14
15
16
17
18
19
20
21
22
23
24
25
26
27
28
29
30
31
32
33
34
35
36
37
38
39
40
41
42
43
44
45
46
47
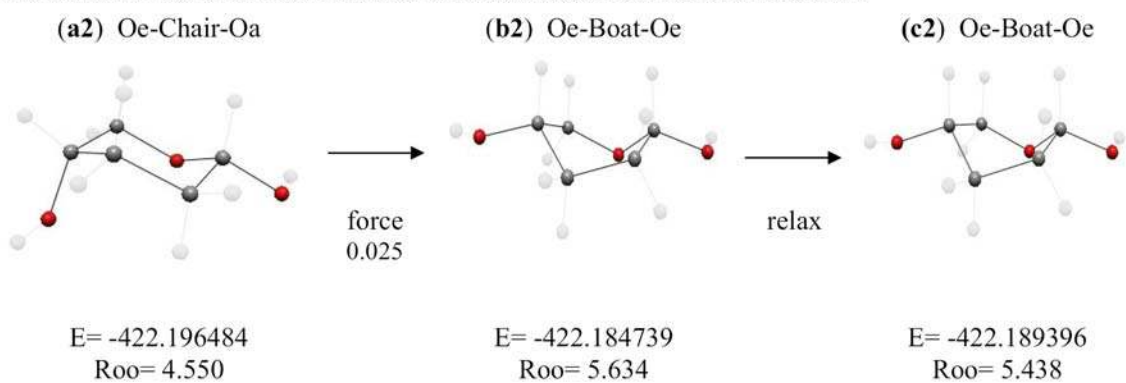48
49
50
51
52
53
54
55
56
57
58
59
60

21. T. Hugel, N. B. Holland, A. Cattani, L. Moroder, M. Seltz and H. E. Gaub, *Science* **296** (2002) 1103

22. J. Baker, A. A. Jarzecki and P. Pulay, *J.Phys.Chem. A* **102** (1998) 1412

23. M. T. Ong, J. Leiding, H. Tao, A.M. Virshup, T. J. Martinez, *J. Am. Chem. Soc.,* (2009), **131**, 6377

24. J. Ribas-Arino, M. Shiga, D. Marx, *Angew. Chem. Int. Ed.*, (2009), **48**, 4190

23

The figure captions

Figure 1. Enforced transitions and inversion in monomers followed by relaxation

    (a1) Oa-Chair-Oe → (b1) Oe-Boat-Oe → (c1) Oe-Boat-Oe (relaxed)
    (a2) Oe-Chair-Oa → (b2) Oe-Boat-Oe → (c2) Oe-Boat-Oe (relaxed)
    (a3) Oe-Chair-Oa → (b3) Oe-Chair-Oe → (c3) Oe-Chair-Oe (relaxed)

    Forces and energies (E) in au, distance between glycosidic oxygens (Roo) in Å.

Figure 2. Enforced transitions and inversion in dimers followed by relaxation

    (a1) → (b1) → (c1)

    (a1) Oa-Chair-aOa-Chair-Oa →
    (b1) Oe-Chair-eOe-Chair-Oe →
    (c1) Oe-Chair-eOe-Chair-Oe (relaxed)

    (a2) → (b2) → (c2) → (d2)

    (a2) Oa-Boat-aOa-Chair-Oa →
    (b2) Oe-Chair-eOa-Chair-Oa →
    (c2) Oe-Chair-eOe-Chair-Oe →
    (d2) Oe-Chair-eOe-Chair-Oe (relaxed)

    (a3) → (b3) → (c3) → (d3)

    (a3) Oa-Boat-aOa-Boat-Oa →
    (b3) Oa-Boat-aOe-Chair-Oe →
    (c3) Oe-Chair-eOe-Chair-Oe →
    (d3) Oa-Boat-aOa-Boat-Oa (relaxed)

    Forces and energies (E) in au, distance between glycosidic oxygens (Roo) in Å.

Figure 3. Structures obtained by the application of external forces along the line joining pairs
    of different ring atoms in *cis*-azobenzene (see Table 1)

Figure 4. Simulated IR spectra of *trans*- and *cis*-azobenzene and the seven new isomers

Figure 5. Simulated Raman spectra of *trans*- and *cis*-azobenzene and the seven new isomers

Figure 6. Simulated VCD spectra of *cis*-azobenzene and the seven new isomers

24

1
2
3
4
5
6
7
8
9
10
11
12
13
14
15
16
17
18
19
20
21
22
23
24
25
26
27
28
29
30
31
32
33
34
35
36
37
38
39
40
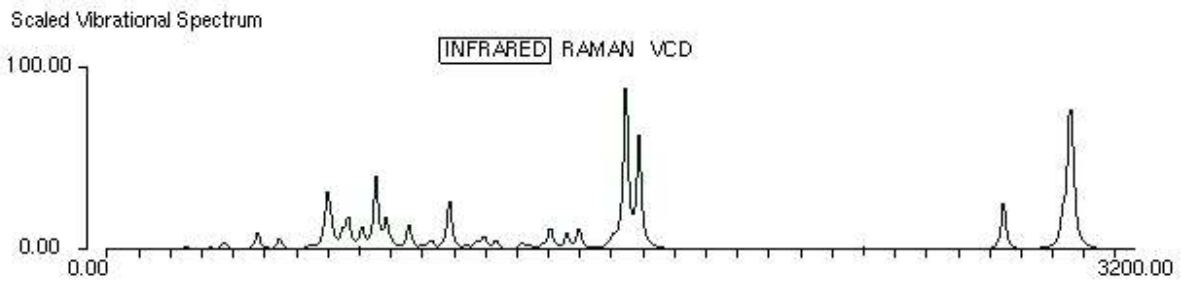41
42
43
44
45
46
47
48
49
50
51
52
53
54
55
56
57
58
59
60

25

Figure 1.

The monomer Oa-Chair-Oe. Enforced transition to Oe-Boat-Oe and relaxation.

(a1) Oa-Chair-Oe

(b1) Oe-Boat-Oe

(c1) Oa-Boat-Oa

force
0.025

relax
inversion

E= -422.201110
Roo= 4.576

E= -422.183441
Roo= 5.690

E= -422.194098
Roo= 4.652
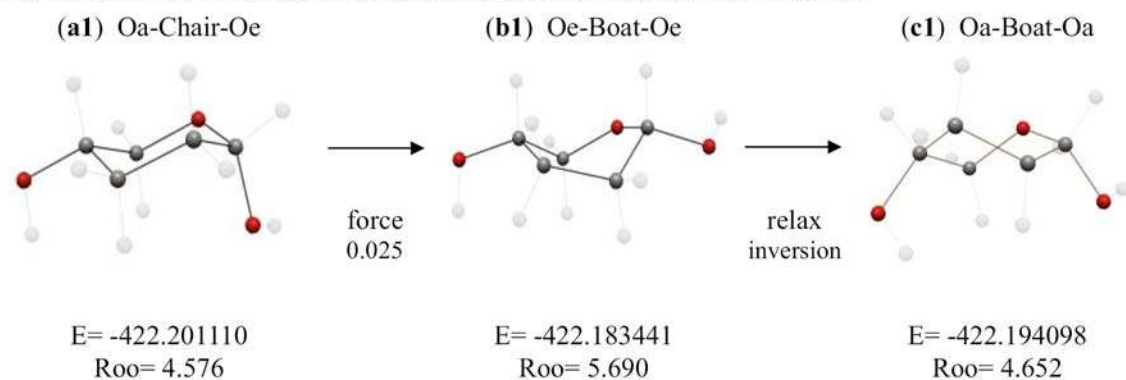
The monomer Oe-Chair-Oa. Enforced transition to Oe-Boat-Oe and relaxation.

(a2) Oe-Chair-Oa

(b2) Oe-Boat-Oe

(c2) Oe-Boat-Oe

force
0.025

relax

E= -422.196484
Roo= 4.550

E= -422.184739
Roo= 5.634

E= -422.189396
Roo= 5.438

The monomer Oa-Chair-Oa. Enforced inversion to Oe-Chair-Oe and relaxation.

(a3) Oa-Chair-Oa

(b3) Oe-Chair-Oe

(c3) Oe-Chair-Oe

force
0.050

relax

E= -422.193814
Roo= 4.521

E= -422.177373
Roo= 5.924

E= -422.197512
Roo= 5.521

26
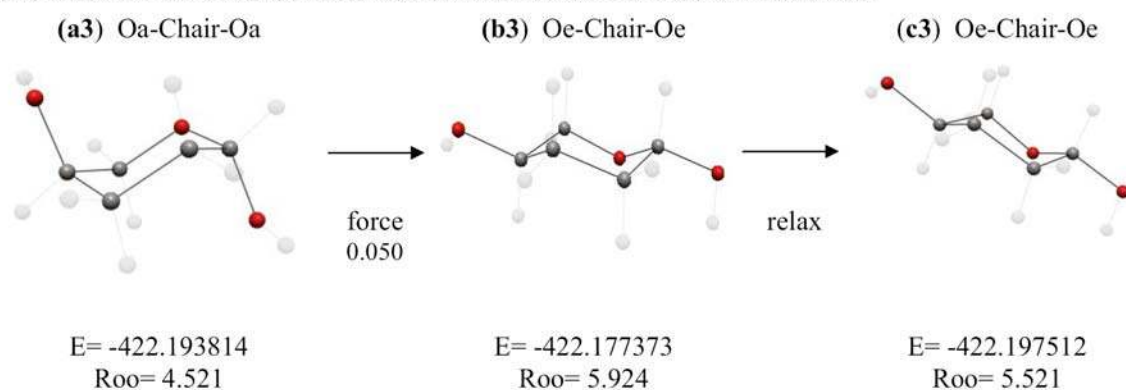
Figure 2. The dimer Oa-Chair-aOa-Chair-Oa. Enforced one-step transition to Oe-Chair-Oe-Chair-Oe and relaxation.

The dimer Oa-Boat-aOa-Chair-Oa. Enforced two-step transition to Oe-Chair-eOe-Chair-Oe and relaxation.

The dimer Oa-Boat-Oa-Boat-Oa. Enforced two-step transition to Oe-Chair-eOe-Chair-Oe and relaxation to Oa-Boat-Oa-Boat-Oa.

(**a1**) Oa-Chair-Oa-Chair-Oa

E=-767.982095, Roo=8.693

(**b1**) Oe-Chair-Oe-Chair-Oe

E=-767.928278, Roo=11.782

(**c1**) Oe-Chair-Oe-Chair-Oe

E=-767.986755, Roo=10.392

force 0.057

relax

(**a2**) Oa-Boat-Oa-Chair-Oa

E=-767.983948, Roo=5.358

(**b2**) Oe-Chair-eOa-Chair-Oe

E=-767.973070, Roo=9.978

(**c2**)Oe-Chair-eOe-Chair-Oe

E=-767.932233, Roo=11.656

(**d2**) Oe-Chair-Oe-Chair-Oe

E=-767.978017,

force 0.004

force 0.050

relax

(**a3**) Oa-Boat-Oa-Boat-Oa

E=-767.976499, Roo=2.966

(**b3**) Oa-Boat-aOe-Chair-Oa

E=-767.976532, Roo=7.857

(**c3**) Oe-Chair-eOe-Chair-Oe

E=-767.967163, Roo=10.644

(**d3**) Oa-Boat-Oa-Boat-Oa

E=-767.984622, Roo=5.058

force 0.002

force 0.005

relax

27

Figure 3. Structures obtained by the application of external forces along the line joining pairs of different ring atoms in *cis*-azobenzene (see Table 1)
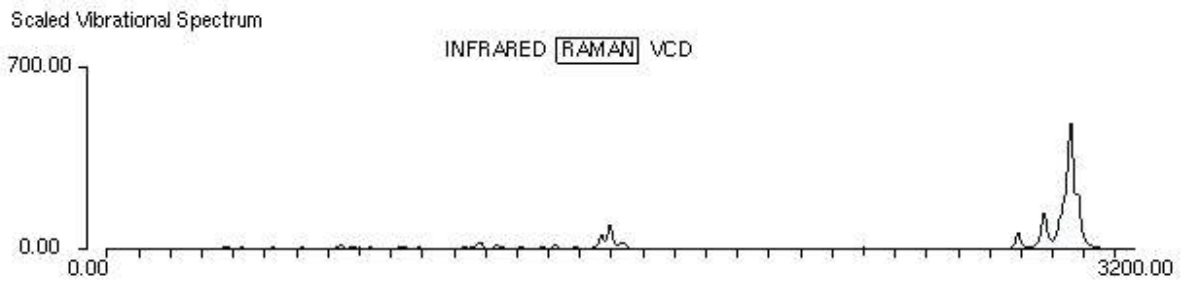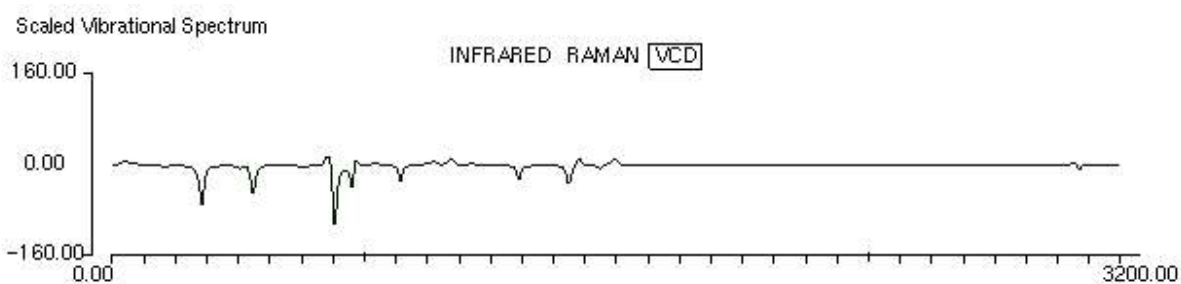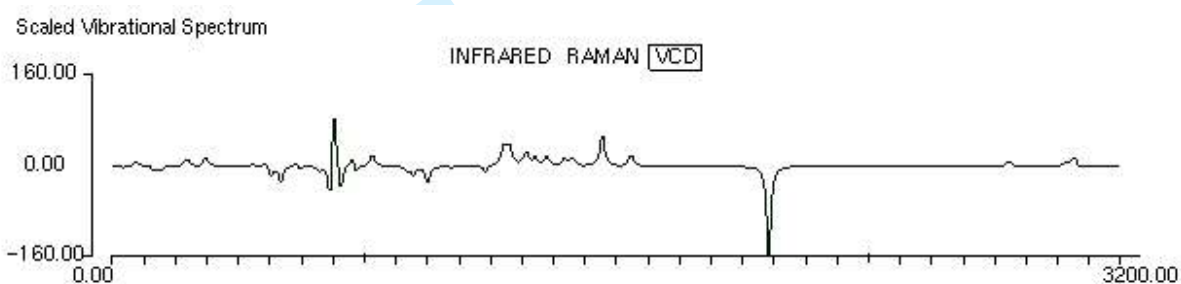

(a) C2-C15

28

1
2
3
4
5
6
7
8
9
10
11
12
13
14
15
16
17
18
19
20
21
22
23
24
25
26
27
28
29
30
31
32
33
34
35
36
37
38
39
40
41
42
43
44
45
46
47
48
49
50
51
52
53
54
55
56
57
58
59
60
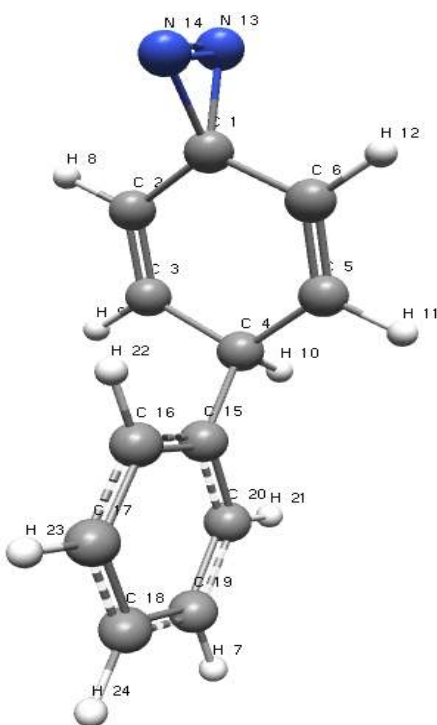
(b) C4-C15 (C_s symmetry)
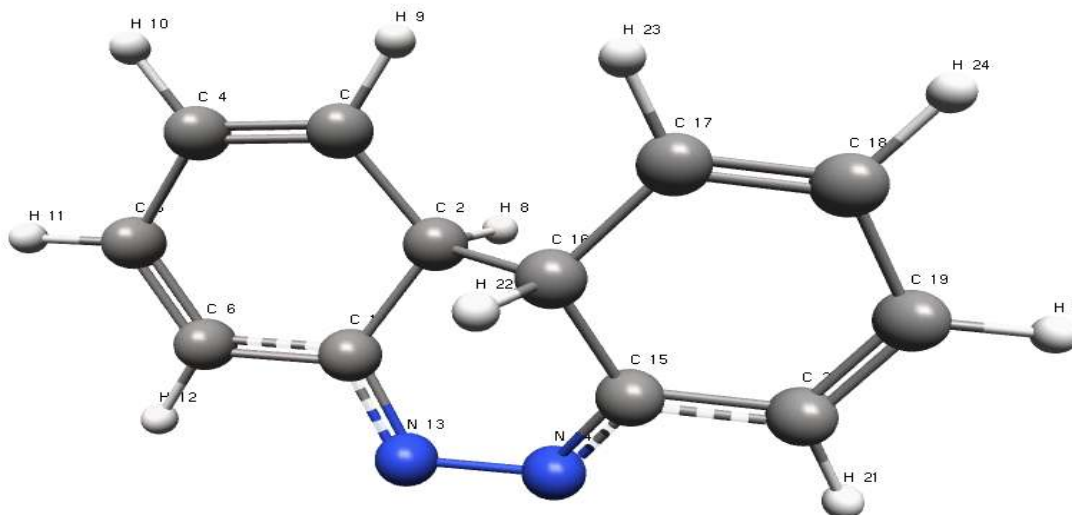
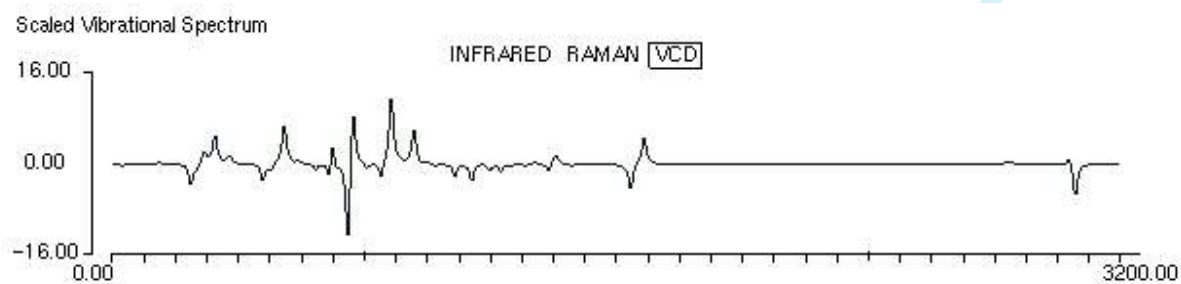
(c) C2-C16 (C_2 symmetry)
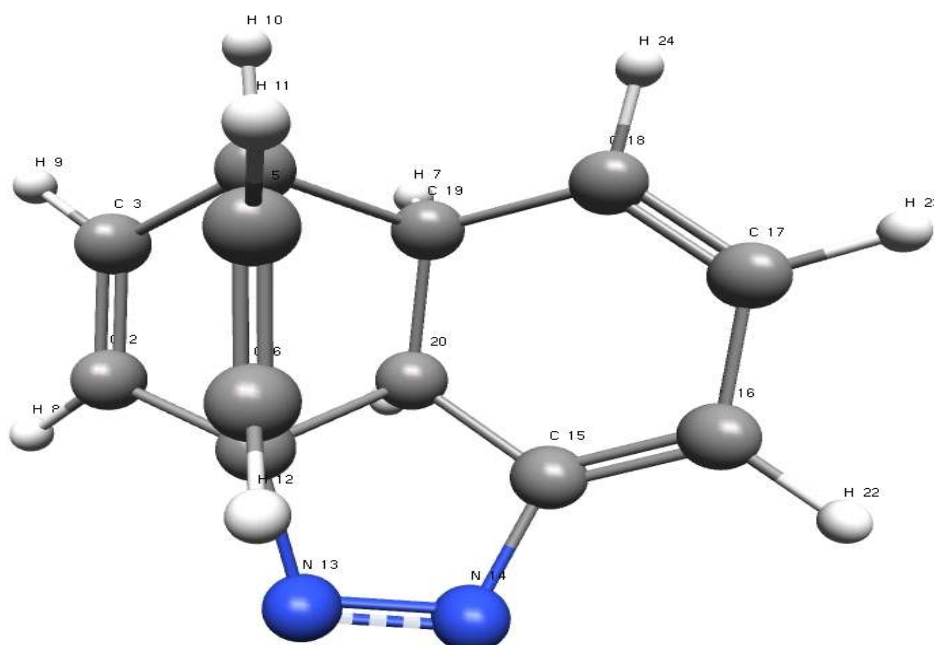
(d) C4-C19
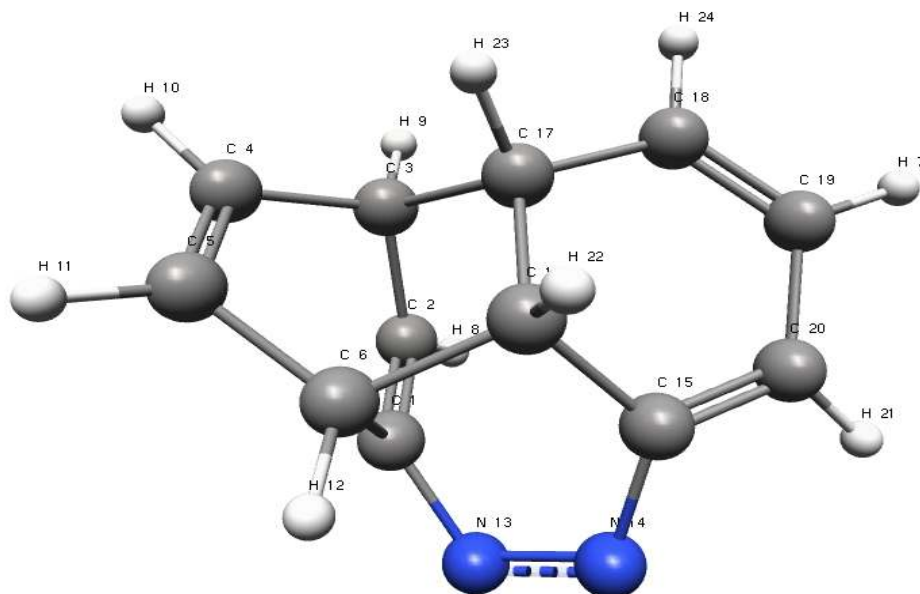
29

(e) C3-C17

(f) C4-C20

30

(g) C3-C20

31
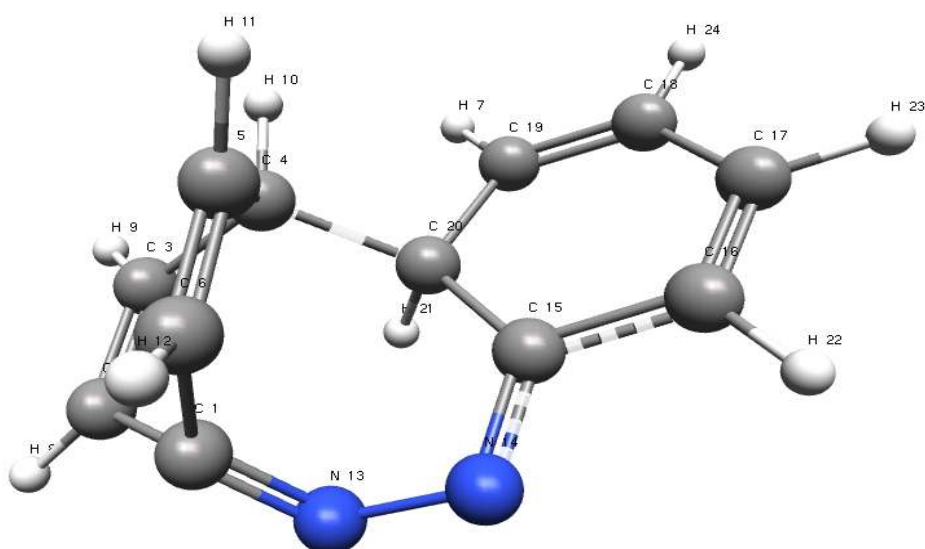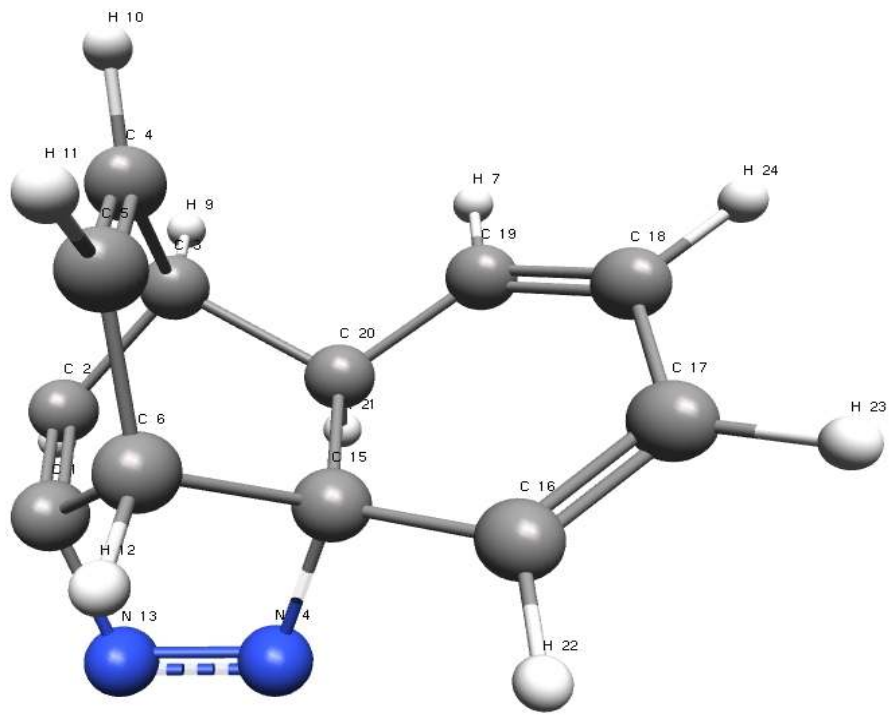
Figure 4 Simulated IR spectra of *trans*- and *cis*-azobenzene and the seven new isomers
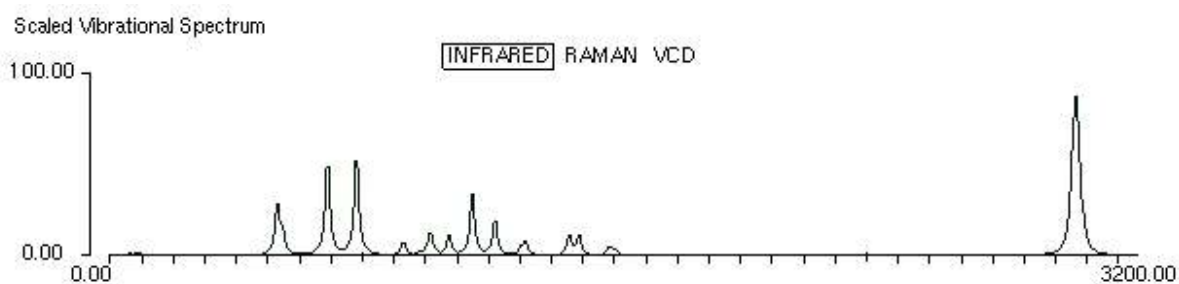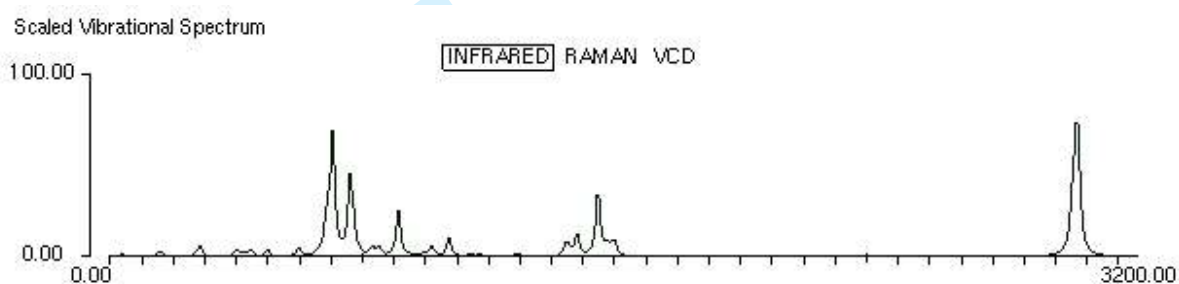
(a) *trans*-azobenzene

(b) *cis*-azobenzene
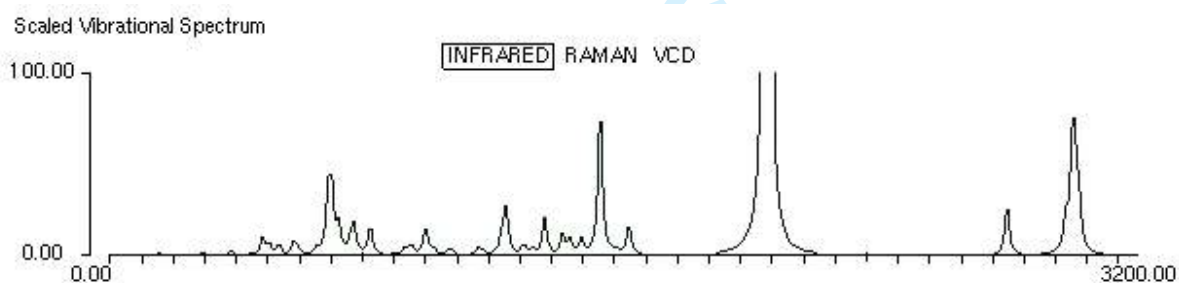
(c) C2-C15 – same intensity scale as all the other simulated IR spectra
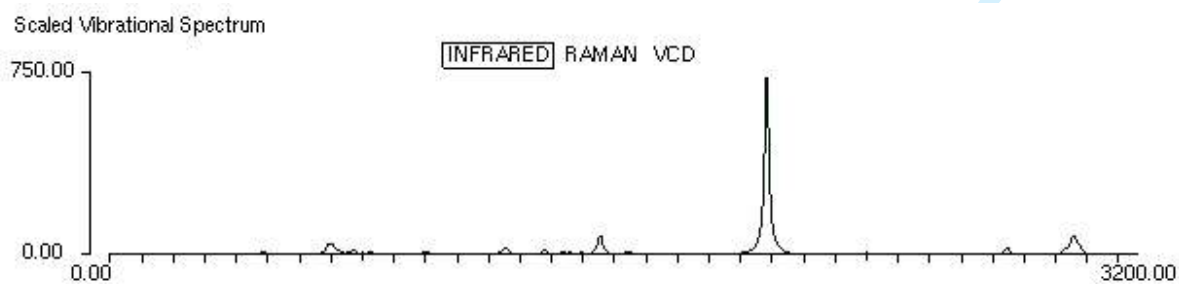
(c) C2-C15 – expanded intensity scale showing very intense IR-active band at 2083 cm^{-1}
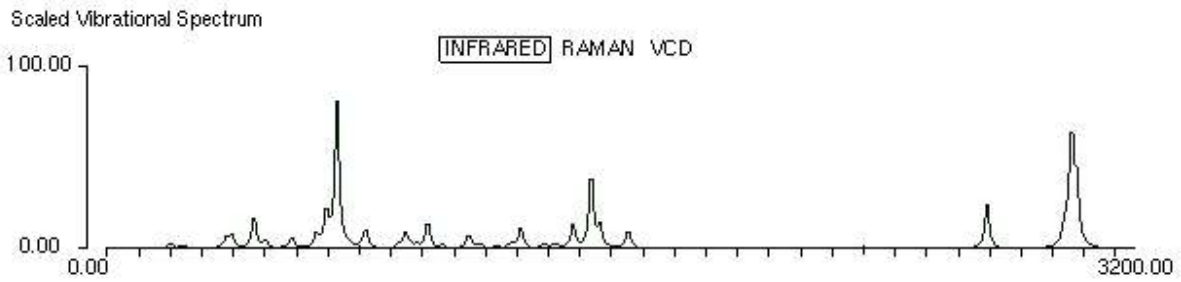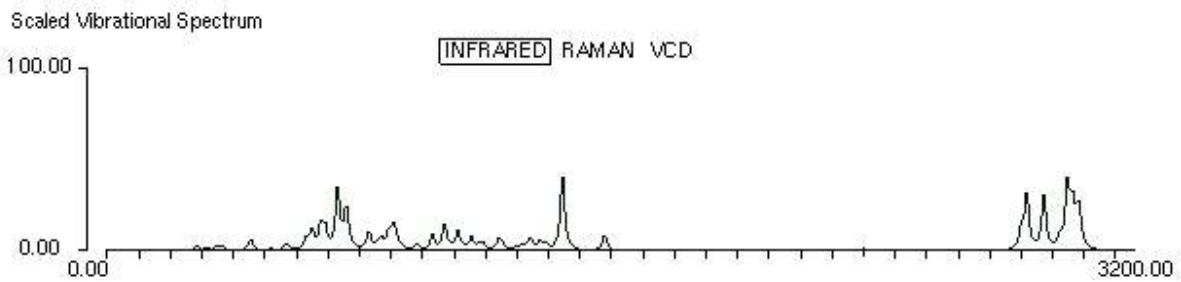
32

(d) C4-C15

(e) C2-C16

(f) C4-C19
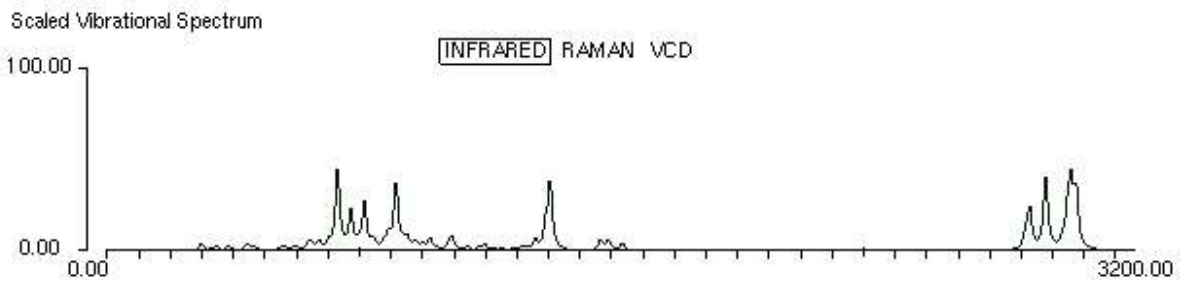
(g) C3-C17
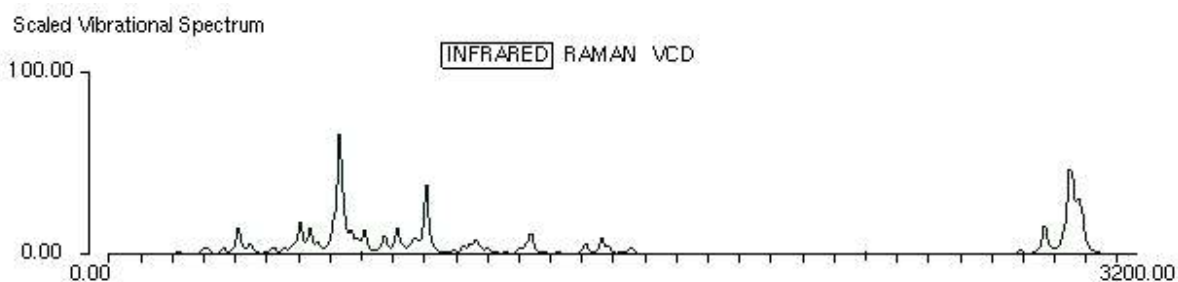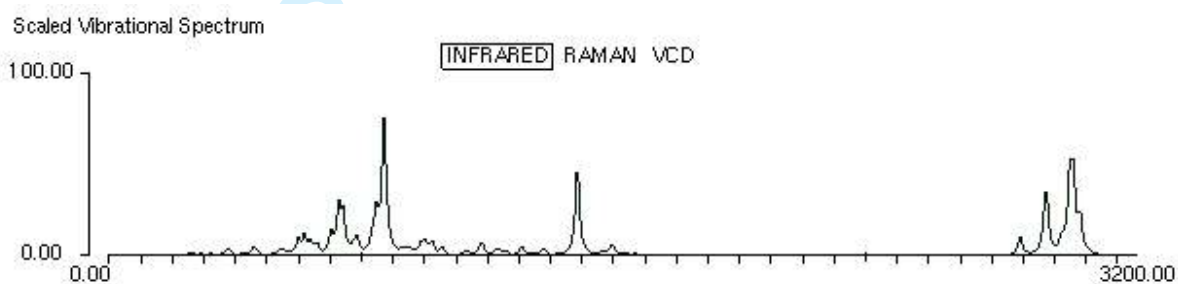
33

(h) C4-C20

(i) C3-C20

34

Figure 5 Simulated Raman spectra of *trans*- and *cis*-azobenzene and the seven new isomers
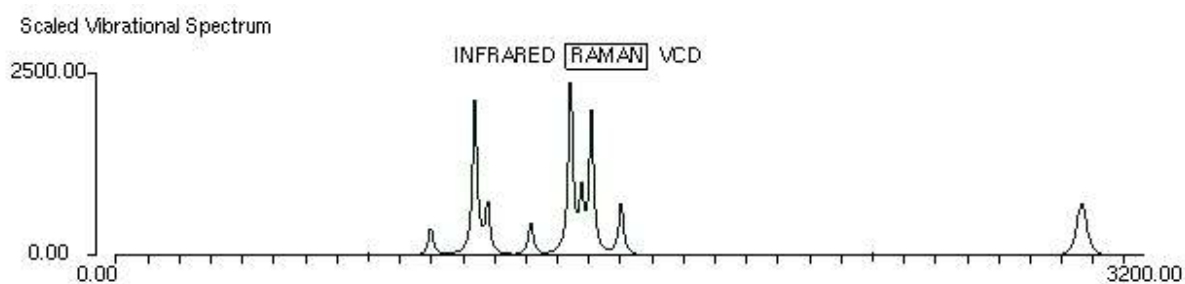
(a) *trans*-azobenzene – expanded intensity scale
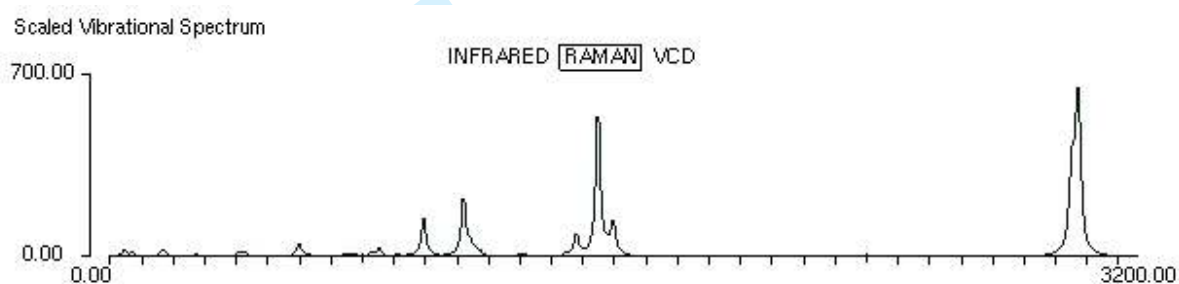
(b) *cis*-azobenzene
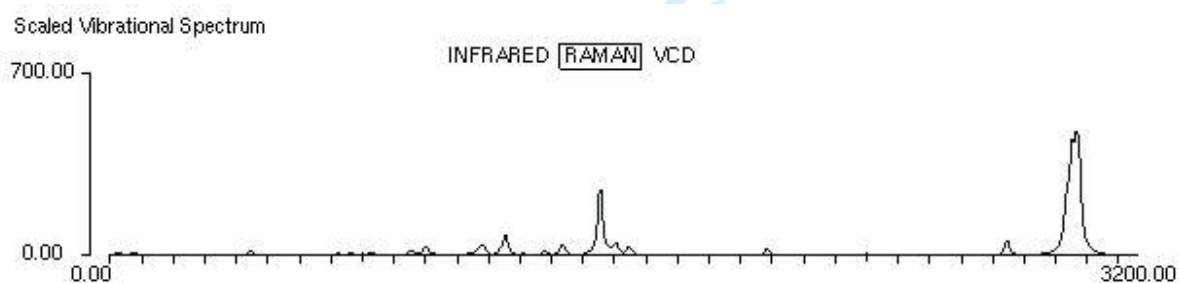
(c) C2-C15
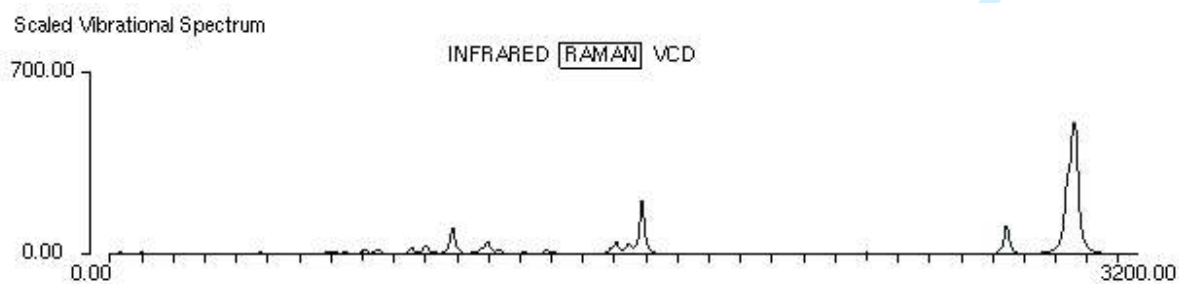
(d) C4-C15
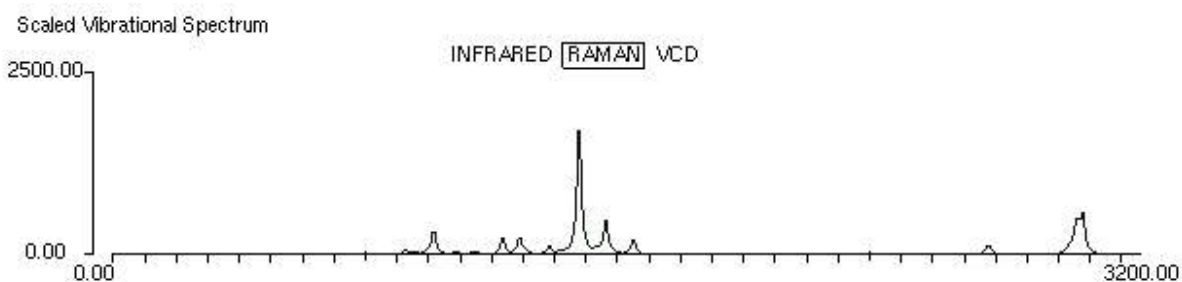
35

(e) C2-C16 – expanded intensity scale showing very intense Raman band at 1478 cm^{-1}
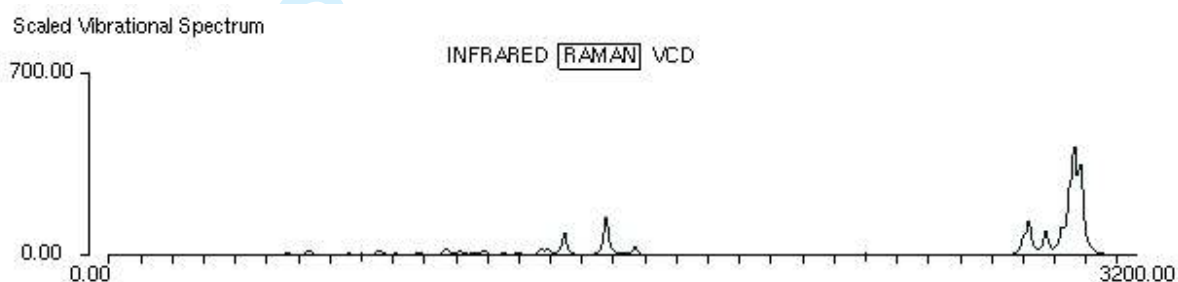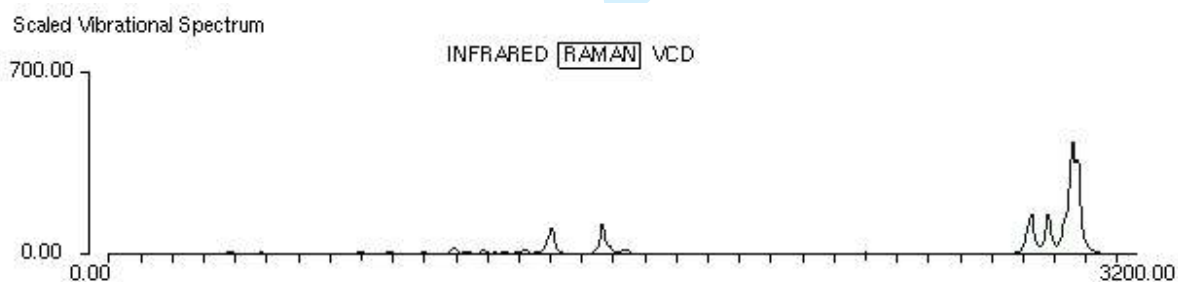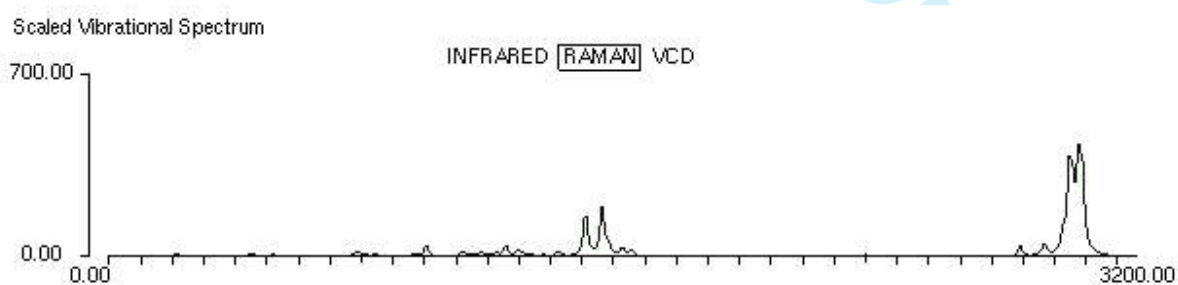
(f) C4-C19

(g) C3-C17

(h) C4-C20

36

1
2
3
4
5
6
7
8
9
10
11
12
13
14
15
16
17
18
19
20
21
22
23
24
25
26
27
28
29
30
31
32
33
34
35
36
37
38
39
40
41
42
43
44
45
46
47
48
49
50
51
52
53
54
55
56
57
58
59
60

Scaled Vibrational Spectrum   INFRARED [RAMAN] VCD

(i) C3-C20

Figure 6 Simulated VCD spectra of *cis*-azobenzene and the seven new isomers

(b) *cis*-azobenzene

(c) C2-C15
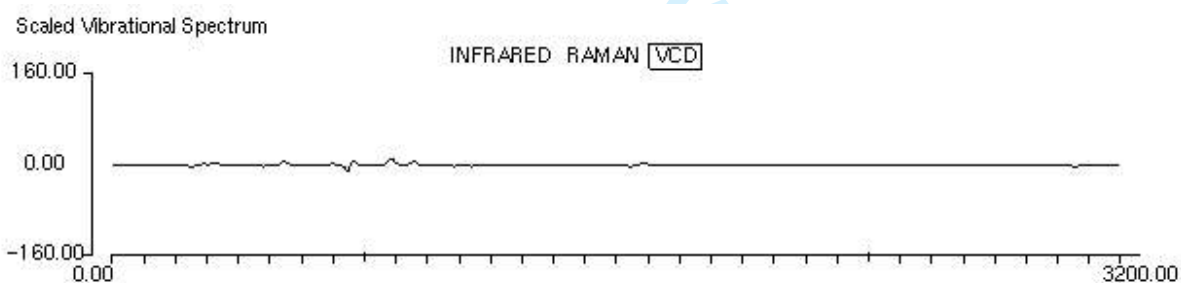
(d) C4-C15 – same intensity scale as all the other simulated VCD spectra
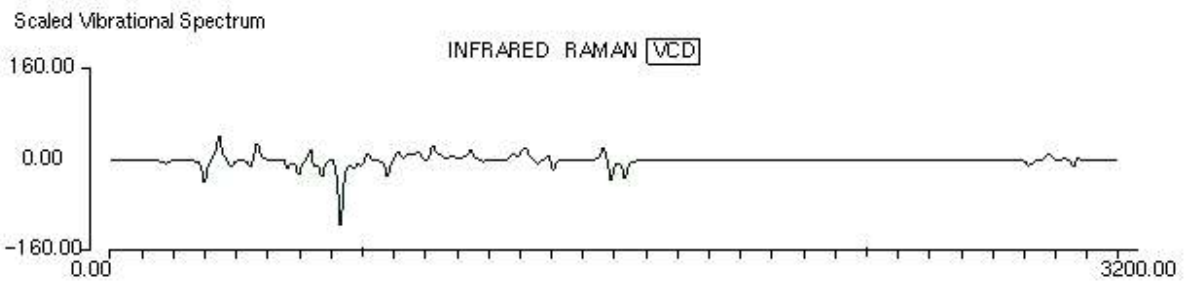

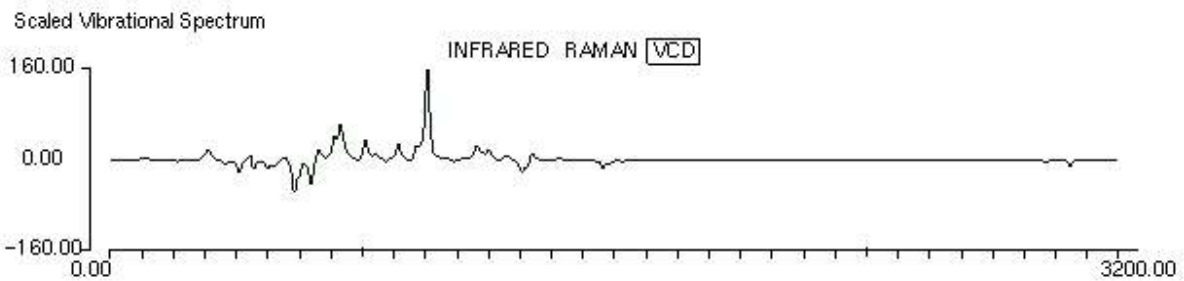(d) C4-C15 – a much reduced intensity scale showing more detail
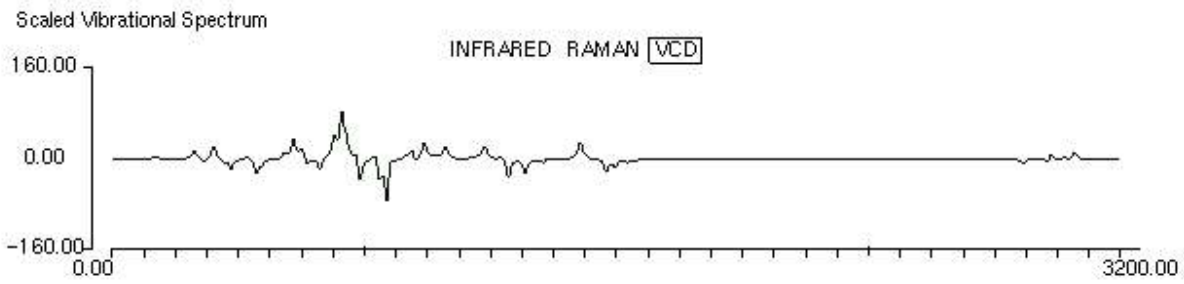
38

(e) C2-C16

(f) C4-C19

(g) C3-C17

(h) C4-C20

Scaled Vibrational Spectrum

INFRARED RAMAN VCD

160.00

0.00

-160.00

0.00   3200.00

(i) C3-C20

40